Electrocatalysis (2020) 11:347–353
https://doi.org/10.1007/s12678-020-00593-z

ORIGINAL RESEARCH

Hydrogen Evolution Reaction on Iridium-Modified Nickel Foam Surfaces

Mateusz Luba[1] · Tomasz Mikolajczyk[1] · Boguslaw Pierozynski[1]

Published online: 8 March 2020
© The Author(s) 2020

Abstract

This work reports on cathodic hydrogen evolution reaction (HER), studied on Ir-activated nickel foam materials, prepared through spontaneous and electrodeposition methods (examined in 0.1 M NaOH electrolyte). Both Ir modifications of Ni foam caused substantial improvement of the HER kinetics, as compared with those recorded for as-received and surface-activated nickel foam materials. Electrochemical examinations were conducted through AC impedance spectroscopy and quasi-steady-state cathodic polarization experiments. Significance of catalytic nature of Ir deposit and employed deposition methodology on the HER behavior of such-obtained Ni foam/Ir composites were discussed in detail by means of SEM/EDX spectroscopy analysis.

Keywords Ni foam · Ir modification · HER · Impedance spectroscopy

Introduction

Electrochemical cathodic generation of H_2 on metal-based catalysts makes hydrogen gas of superior purity and importance as an energy carrier for PEM (proton-exchange membrane) fuel cell and for heating purposes. The nickel element itself is well-known as a highly reactive catalyst for hydrogen evolution reaction (HER) in alkaline media, where it also possesses outstanding corrosion resistance. Of special importance from electrochemistry point of view are structures having a large specific surface area, including nickel foam–based catalysts. These materials make not only high porosity and large specific surface area but also catalysts having exceptionally beneficial (for the purpose of this investigation) electrical conductivity and mechanical characteristics [1–6].

Substantial enhancement of electrocatalytic HER behavior of nickel foam could generally be done by surface deposition of nano-structured noble metal elements. The above could be conducted through electrodeposition, spontaneous deposition [5, 7, 8], or by chemical reduction processes, where the latter is usually conducted with sodium borohydride, ethylene glycol, hydrazine, and their mixtures [9–13].

In this paper, the HER behavior of iridium-activated nickel foam (obtained through spontaneous and electrodeposition methods) is presented, also in comparison with similar works published from this laboratory, on catalytically (Pd, Ru, and Pt) activated Ni foam samples [14–17].

Research Highlights
- Ir deposition radically enhanced HER kinetics of Ni foam.
- Ir modifies electrochemically active surface of nickel foam.
- Ir-activated Ni foam cathodes for alkaline water electrolysers.

✉ Boguslaw Pierozynski
bogpierozynski@yahoo.ca; boguslaw.pierozynski@uwm.edu.pl

[1] Department of Chemistry, Faculty of Environmental Management and Agriculture, University of Warmia and Mazury in Olsztyn, Plac Lodzki 4, 10-727 Olsztyn, Poland

Experimental

Chemicals, Solutions, Electrochemical cell, and Electrodes

All solutions were prepared from ultra-pure water, generated by Direct-Q3 UV water purification system from Merck (18.2 MΩ cm water resistivity). A 0.1 M sodium hydroxide solution was prepared from AESAR, 99.996% NaOH pellets, and 0.5 M H_2SO_4 (SEASTAR Chemicals, BC, Canada) solution was used for periodic charging of a Pd reversible hydrogen electrode. In this work, a three-compartment, pyrex-glass made electrochemical cell was employed. In a central part, a Ni foam–based working electrode (WE) was placed, whereas both Pd reference hydrogen electrode (RHE) (as reference) and a Pt counter electrode (CE) were positioned in separate compartments equipped with joint stopcocks (with openings),

where the reference one was additionally furnished with a Luggin capillary.

Nickel foam was purchased from the MTI Corporation (purity > 99.99% Ni; thickness 1.6 mm; surface density 346 g m^{-2}; porosity ≥ 95%; estimated electrochemically active surface 14.9 cm^2 [14]). Electrochemical measurements were conducted on four types of Ni foam–based catalyst (ca. 1.1 × 1.1 cm samples), namely:

a) As-received Ni foam (acetone wash/ultrasonication 900 s at 298 K + air drying),
b) Etched Ni foam (acetone wash/ultrasonication 900 s at 298 K + air drying followed by 2 M HCl acid etching 900 s at 333 K + ultra-pure water rinsing + air drying),
c) Etched, Ir-modified nickel foam by spontaneous [18–20] deposition upon ultrasonication (0.1 M HCl + 1×10^{-3} M $IrCl_3$ (Sigma Aldrich, pure p.a.), 298 K at 30 s and 300 s), and
d) Etched, Ir-modified nickel foam by electrodeposition [21] upon ultrasonication (0.5 M H_2SO_4 + 1×10^{-3} M $IrCl_3$ (Sigma Aldrich, pure p.a.), 298 K for j_{cat} = 0.08 mA cm^{-2} at 600 s and j_{cat} = 5.25 mA cm^{-2} at 1200 s).

Methodology

Electrochemical AC impedance spectroscopy (EIS) and quasi-steady-state polarization techniques were employed in this work. All electrochemical tests were conducted at room temperature (298 ± 1 K) by the *Solartron* 12,608 W Full Electrochemical System (1260 frequency response analyzer + 1287 electrochemical interface). For the EIS measurements, the generator supplied an output signal of 5 mV rms, and the frequency was swept between 1.0×10^5 and 0.5×10^{-1} Hz. *ZPlot 2.9* and *Corrware 2.9* software packages (Windows, Scribner Associates, Inc.) were employed to monitor the instruments. Generally, three impedance tests were performed at each cathodic potential, for two working samples, where reproducibility of produced results was usually about 10%. Data analysis was carried out by means of *ZView 2.9* (*Corrview 2.9*) software packs, where the impedance spectra were fitted with a complex, non-linear, least-squares immittance fitting program, *LEVM 6*, written by J.R. Macdonald [22]. Furthermore, quasi-steady-state cathodic polarization experiments for the HER were conducted on selected Ni foam and Ir-activated nickel foam electrodes (performed at a sweep rate of 0.5 mV s^{-1}). Conversely, SEM/energy-dispersive X-ray (EDX) surface spectroscopy characterization of all examined Ni foam and iridium-modified Ni foam samples was carried out by means of Merlin FE-SEM microscope (Zeiss), equipped with Bruker XFlash 5010 EDX instrumentation (with 125 eV resolution).

Results and Discussion

SEM/EDX Characterization of Nickel Foam and Ir-Modified Ni Foam Electrodes

Figure 1a below presents the SEM micrograph picture of MTI-manufactured nickel foam, at × 25,000 magnification. Consequently, Fig. 1b illustrates the foam etching effect with characteristic grooves visible on the Ni foam surface at the corresponding magnification. On the other hand, Fig. 1 c and d demonstrate the effect of electrodeposition of iridium at current-densities of 0.08 and 5.25 mA cm^{-2} on the MTI foam, recorded at the same magnification. Here, iridium formed quite homogeneously distributed deposits, without any visible difference between Ir loadings. Furthermore, Fig. 1 e and f show the result of spontaneous deposition of iridium on the Ni foam surface for immersion time of 30 s and 300 s, at × 25,000 magnification, correspondingly. Similarly to electrodeposits, spontaneous iridium deposits also formed evenly distributed structures (X-ray diffraction showed clear presence of Ir phase on the diffractogram, but the equipment was practically operated at its detection limit; respective figure is not shown in this work).

Simultaneously, EDX spectra illustrated in Fig. 1 c through f correspond to electrodeposited (c and d) and spontaneously deposited iridium (e and f) on the Ni foam electrode surfaces. Most importantly, very homogeneous distribution of iridium over the surface of Ni foam substrate allowed for precise, fairly quantitative determination of the Ir element content in the studied composites. Hence, an average content of the Ir deposits came to 0.1, 1.2, 0.3, and 0.3 wt.% for ED 1 (electrodeposited iridium 298 K, j_{cat} = 0.08 mA cm^{-2} at 600 s), ED 2 (electrodeposited iridium 298 K, j_{cat} = 5.25 mA cm^{-2} at 1200 s), SD 1 (spontaneously deposited iridium 298 K at 30 s), and SD 2 (spontaneously deposited iridium 298 K at 300 s) Ni foam/Ir samples, respectively.

Electrochemical Impedance Characterization

EIS characterization of the HER on pure (as received), etched, spontaneously Ir-activated, and Ir-modified by means of iridium electrodeposition on the surface of Ni foam electrodes in 0.1 M sodium hydroxide is shown in Figs. 2 and 3, and Table 1. Hence, all impedance-tested, Ni foam samples exhibited single, "depressed" semicircles in relation to a single-step charge-transfer reaction at all studied potentials, over the examined frequency range (examples of Nyquist impedance plots derived at − 100 mV are shown in Fig. 2 a and b). However, a typical electrode porosity response, evidenced through the appearance of a high-frequency semicircle was practically undetectable in

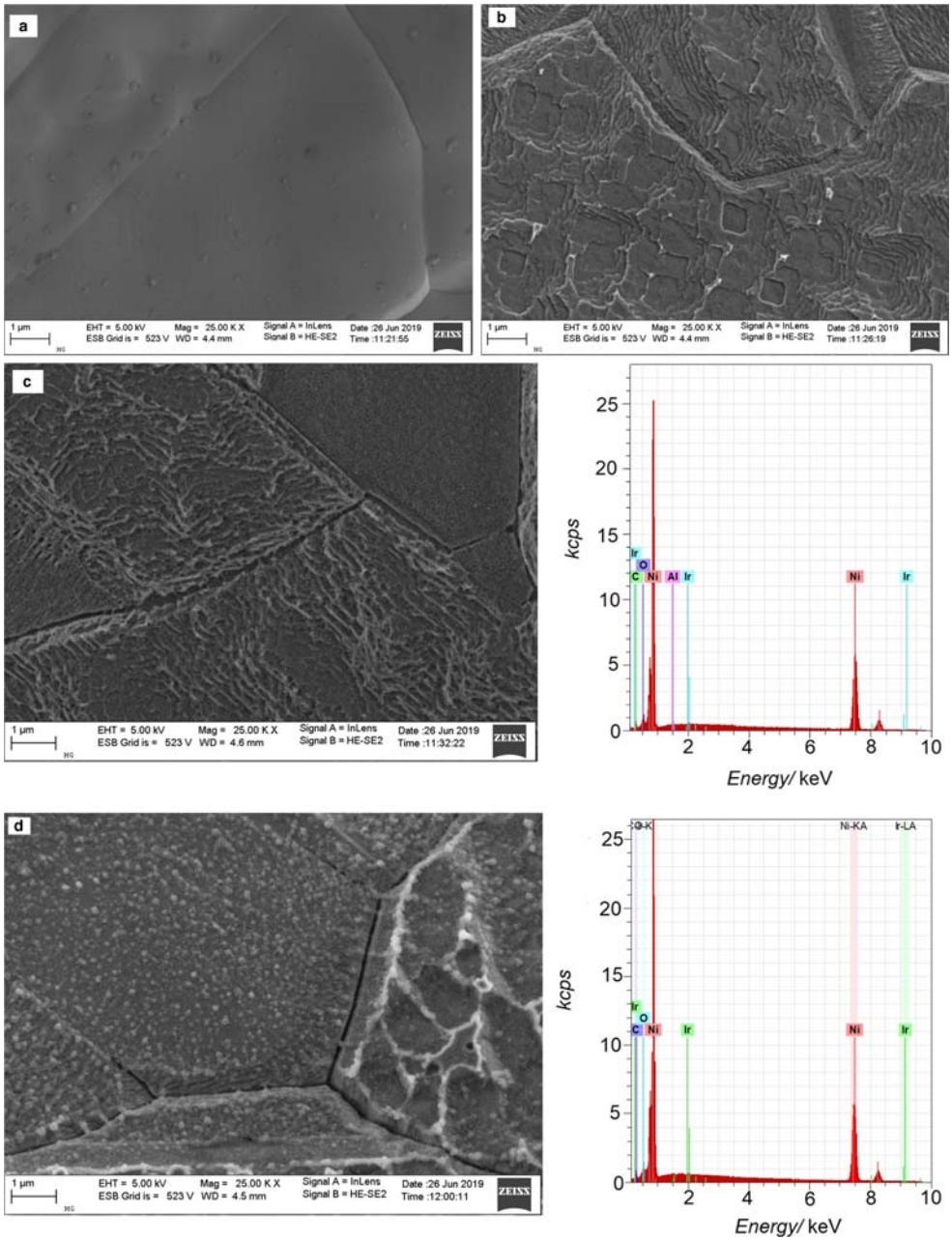

Fig. 1 **a** SEM micrograph picture of as-received Ni foam surface, taken at × 25,000 magnification. **b** As above, but etched Ni foam surface. **c** SEM micrograph picture of ED 1 Ni foam/Ir sample, taken at × 25,000 magnification and EDX pattern. **d** As **c**, but for ED 2 Ni foam/Ir surface. **e** As **c**, but for SD 1 Ni foam/Ir surface. **f** As **c**, but for SD 2 Ni foam/Ir surface

the impedance plots. Then, the overpotential dependence of the Faradaic reaction resistance (R_{ct}) parameter and capacitance variable T, which approximates double-layer capacitance (C_{dl}) parameter, for the HER (recorded based on a constant phase element—CPE-modified Randles equivalent circuit presented in Fig. 3) is shown in Table 1. The CPE element is generally included in the equivalent circuit in order to account for the capacitance dispersion [23, 24] effect, represented by somewhat deformed semicircles in the Nyquist impedance plots (see Fig. 2 again).

Hence, for the etched Ni foam electrode, the recorded R_{ct} parameter became radically reduced from 923 Ω cm^2 at −100 mV to 42 Ω cm^2 at −400 mV vs. RHE (compare with 1220 vs. 60 Ω cm^2 for the as-received nickel foam sample, also with similar results presented by Pierozynski et al. in Table 1 of Ref. [14]). Simultaneously, at two potential extremes, the derived T parameter values came to 120.7 and 46.5 μF cm^{-2} s$^{\varphi-1}$, and 20.4 and 13.2 μF cm^{-2} s$^{\varphi-1}$ for the etched and the as-received Ni foam samples, correspondingly (Table 1). The above behavior is clearly indicative of a remarkable role that the catalyst's surface

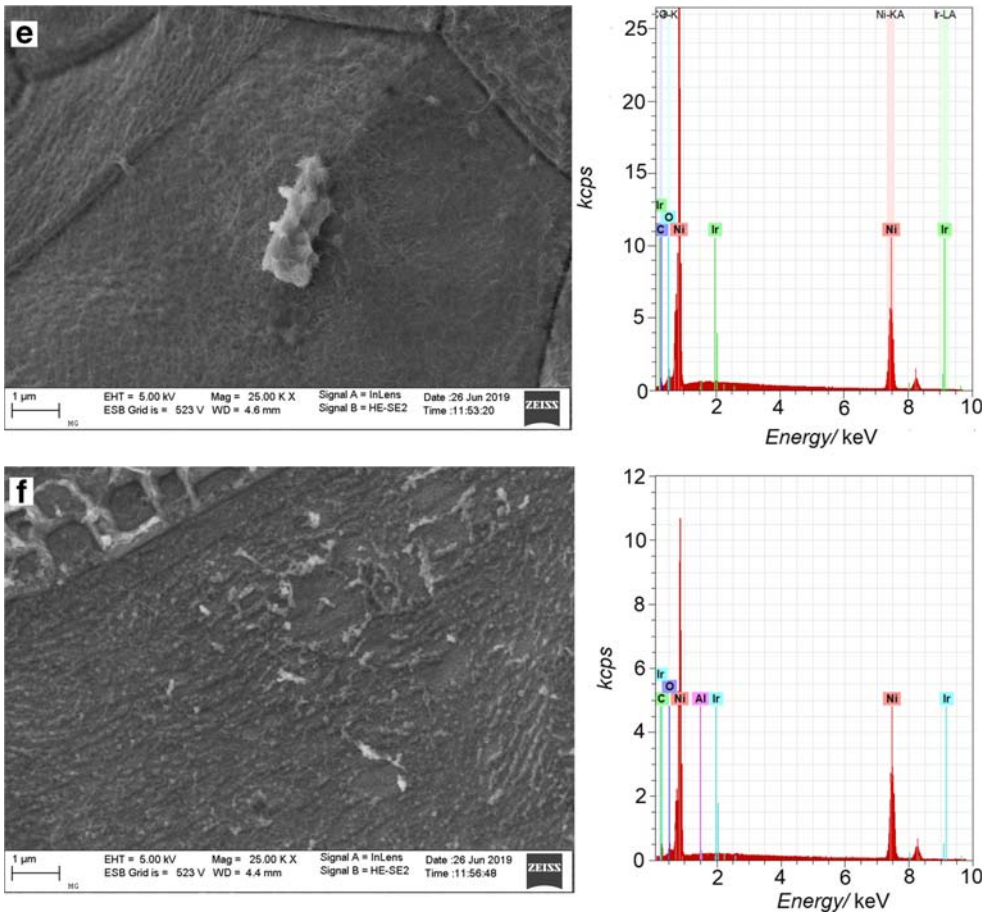

Fig. 1 (continued)

development plays in enhancing its electrocatalytic properties (nearly 30% reduction of the R_{ct} parameter in relation to 6.2× increase of the derived T value at the potential of − 100 mV). The latter effect could also be evidenced through detailed analysis of the SEM micrograph pictures presented in Fig. 1 a and b.

Substantially enhanced HER catalysis with respect to that of the etched Ni foam surface was recorded on iridium-activated nickel foam electrodes. Specifically, for the spontaneously deposited Ir element under SD 1 conditions (298 K, $t = 30$ s; 0.3 wt.% Ir) on the Ni foam substrate, the R_{ct}

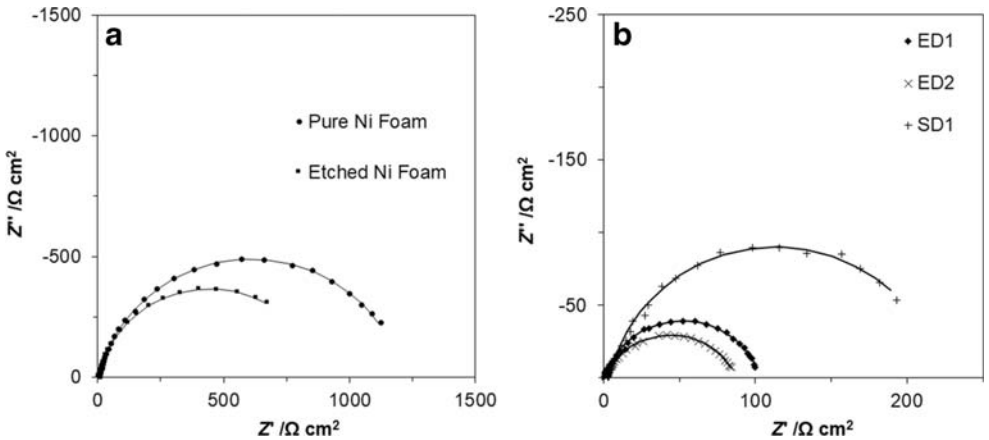

Fig. 2 Complex-plane impedance plots for the HER on **a** pure (as received) and etched Ni foam electrode surfaces in contact with 0.1 M NaOH, recorded at 298 K for the potential of − 100 mV (vs. RHE). The solid lines correspond to the representation of the data according to the equivalent circuit shown in Fig. 3. **b** As above, but recorded on Ir-activated Ni foam via electrodeposition of iridium (ED 1 and ED 2) and spontaneous deposition of Ir (SD 1)

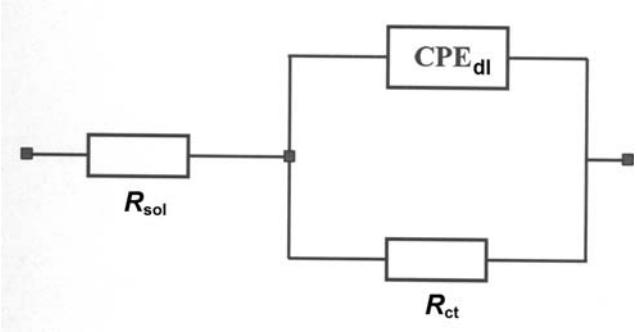

Fig. 3 Equivalent circuit model used for fitting the impedance data for Ni foam and Ir-activated nickel foam electrode surfaces, obtained in 0.1 M NaOH solution. The circuit includes a constant phase element (CPE) for distributed capacitance; R_{ct} and T (as CPE_{dl}) elements correspond to the HER charge-transfer resistance and double-layer capacitance components, and R_{sol} is solution resistance

Table 1 Electrochemical parameters (with their standard deviations) for the HER, obtained on Ni foam (as received and etched) and Ir-modified (spontaneously deposited: SD 1 and SD 2, and electrodeposited: ED 1 and ED 2) Ni foam electrodes in contact with 0.1 M NaOH. The results were obtained by fitting the CPE-modified Randles (Fig. 3) equivalent circuit to the experimentally obtained impedance data (reproducibility typically about 10%, $\chi^2 = 2 \times 10^{-4}$ to 9×10^{-4}); dimensionless φ parameter ranged from 0.83 to 0.96 for η rising from − 100 to − 400 mV vs. RHE

E/mV	R_{ct}/Ω cm^2	T/μF cm^{-2} s$^{\varphi-1}$	R_{ct}/Ω cm^2	T/μF cm^{-2} s$^{\varphi-1}$
	As-received Ni foam		Etched Ni foam	
− 100	1220 ± 3	20.4 ± 0.2	923 ± 8	120.7 ± 2.3
− 150	509 ± 2	19.2 ± 0.3	819 ± 5	90.4 ± 1.2
− 200	273 ± 13	17.8 ± 0.4	400 ± 2	68.7 ± 1.0
− 250	156 ± 10	15.9 ± 0.8	179 ± 1	52.6 ± 1.1
− 300	106 ± 1	15.3 ± 0.9	90 ± 1	47.0 ± 1.6
− 350	79 ± 1	17.4 ± 1.3	58 ± 1	47.8 ± 1.8
− 400	60 ± 1	13.2 ± 0.9	42 ± 1	46.5 ± 2.0
	Ir-activated Ni foam: SD 1		Ir-activated Ni foam: SD 2	
− 100	219 ± 2	77.5 ± 2.7	269 ± 1	75.7 ± 0.9
− 150	215 ± 2	56.0 ± 1.5	192 ± 2	70.1 ± 1.3
− 200	150 ± 1	53.8 ± 1.6	133 ± 1	63.0 ± 1.3
− 250	99 ± 1	52.2 ± 3.1	93 ± 2	53.0 ± 2.6
− 300	66 ± 1	59.5 ± 4.3	66 ± 1	49.4 ± 1.8
− 350	48 ± 1	49.4 ± 3.3	48 ± 1	48.8 ± 2.1
− 400	37 ± 1	45.0 ± 2.1	37 ± 1	45.5 ± 1.8
	Ir-activated Ni foam: ED 1		Ir-activated Ni foam: ED 2	
− 100	102 ± 1	168.5 ± 3.7	87 ± 1	220.4 ± 4.2
− 150	88 ± 1	142.4 ± 4.3	79 ± 1	144.3 ± 3.9
− 200	76 ± 1	132.2 ± 4.3	70 ± 1	135.2 ± 4.0
− 250	61 ± 1	114.9 ± 3.5	61 ± 1	129.6 ± 5.0
− 300	52 ± 1	108.1 ± 4.0	52 ± 1	123.3 ± 4.7
− 350	44 ± 1	99.4 ± 6.6	44 ± 1	104.3 ± 3.1
− 400	47 ± 1	93.6 ± 3.4	36 ± 1	95.2 ± 4.1

parameter reached 219 Ω cm^2 at − 100 mV and 37 Ω cm^2 at − 400 mV vs. RHE, where the recorded values of the interfacial capacitance parameter came to 77.5 and 45.0 μF cm^{-2} s$^{\varphi-1}$ for the respective potential values (considerably reduced capacitance values were derived as compared with those recorded for the etched Ni foam electrode). Significant drop of the capacitance upon overpotential augmentation corresponds to partial blocking of electrochemically available surface area of the electrode by freshly generated H_2 bubbles at increased cathodic overpotentials (also refer to Ref. [14] for details). Interestingly, further extension of Ir deposition time to 300 s (SD 2 sample in Table 1) had practically no influence on the resulted electrocatalytic behavior of the Ni foam/Ir composite. The latter most likely results from the fact that when the Ni foam surface becomes evenly covered by iridium (refer to Fig. 1 e and f), it completely loses its original activity towards spontaneous deposition of noble Ir element.

On the other hand, for the electrochemically deposited iridium (sample ED 1, ca. 0.1 wt.% Ir, 1–2% process efficiency [21]), the process of cathodic evolution of hydrogen becomes significantly facilitated, as compared with that of the spontaneous Ir deposition (sample SD 1). Here, the recorded R_{ct} parameter came to 102 and 47 Ω cm^2 at − 100 and − 400 mV, correspondingly (about 48% reduction of the R_{ct} at the initial examination potential of − 100 mV). On the contrary, the recorded values of the interfacial capacitance parameter came to 168.5 and 93.6 μF cm^{-2} s$^{\varphi-1}$ for the respective potentials (ca. 1.8× increased T parameter at the initial probing potential). Thus, one can draw a conclusion that the above-described HER kinetics facilitation is purely a result of electrochemically active surface area expansion, as recorded for the ED 1 electrode, comparatively with that of the SD 1 sample. Further increase of iridium mass deposited on the Ni foam surface (ED 2 sample, ca. 1.2 wt.% Ir) resulted practically in no additional HER process facilitation, but in a small increase of the electrochemically active surface area (see Table 1 for details).

In addition, the exchange current-density values (j_0) for the HER on the examined Ni foam–based electrodes were derived by utilizing the linear relationship of −log R_{ct} vs. η/overpotential (where η ranged from − 100 to − 400 mV/RHE with 50 mV potential increments, see Fig. 4), fulfilled by kinetically controlled reactions through employing the Butler-Volmer equation and the relation between the j_0 and the R_{ct} parameter for overpotential approaching 0 [25–27]. Hence, the calculated j_0 values came to 5.9×10^{-6} and 3.9×10^{-6} A cm^{-2} for the as-received and etched Ni foam samples, respectively. Significantly increased j_0 values were recorded for iridium-modified nickel foam samples, i.e., 1.3×10^{-5}, 4.6×10^{-5}, and 5.6×10^{-5} A cm^{-2}, respectively, for SD 1, ED 1, and ED 2 electrodes. Presented here, reaction resistance and the impedance-derived exchange current-density results compare fairly well with those previously reported on unmodified and

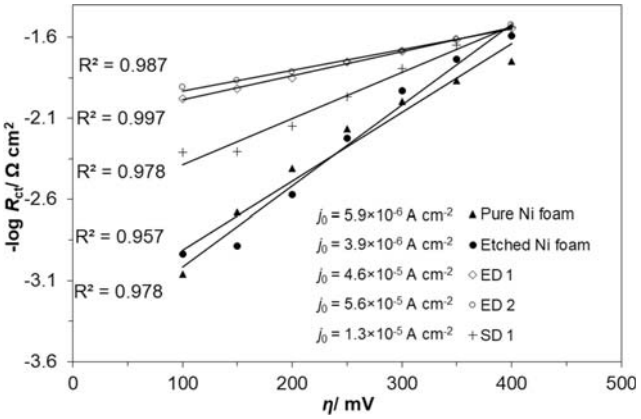

Fig. 4 −log R_{ct} vs. overpotential (η) relationship for the HER, studied in 0.1 M NaOH on Ni foam and Ir-activated nickel foam electrodes (symbols represent experimental results)

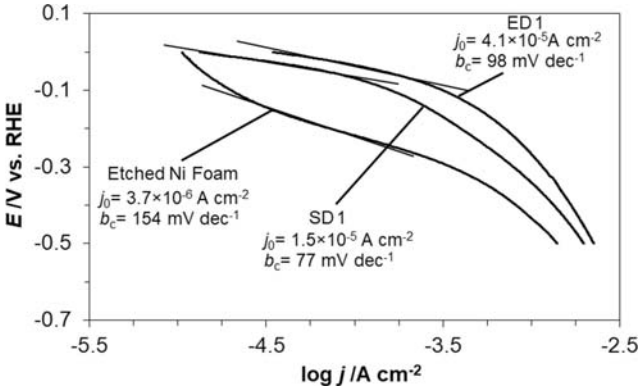

Fig. 5 Quasi-steady-state cathodic polarization curves (recorded at a rate of 0.5 mV s^{-1}) for the HER on etched nickel foam and Ir-activated (ED 1 and SD 1) Ni foam electrode surfaces, carried out in 0.1 M NaOH solution; appropriate *iR* correction was made based on the solution resistance derived from the impedance measurements

Pd (Ru)-activated nickel foam materials from this laboratory [14]. However, in contrast to the very large surface area, nanocatalytic Pd/Ru island deposits described in the latter case, this work utilizes the Ni foam/Ir composites having fairly homogeneously deposited iridium element particles over the Ni foam base. Moreover, Papaderakis et al. [20] examined the process of HER on Ir and Ir-Ni (ca. 80% Ir) bimetallic deposit obtained by a galvanic replacement method. Thus, recorded by these authors, the R_{ct} parameter values for the HER at − 300 mV/SCE (in 0.1 M $HClO_4$) came to 49.37 and 36.74 Ω cm^2 for iridium and Ir-Ni deposit, respectively (compared with 102 Ω cm^2 for the ED 1 sample recorded at − 100 mV/RHE). Also, the reported j_0 values [20] were 2.9×10^{-4} and 4.6×10^{-4} A cm^{-2} for Ir and Ir-Ni electrodes, correspondingly. On the other hand, Sheng et al. [28] reported an exchange current-density value of 8.18×10^{-6} A cm^{-2} on iridium-modified (17.7 wt.%) silicon nanowire structure in 0.5 M H_2SO_4 solution. Finally, Vazquez-Gomez et al. [8] examined the HER behavior of iridium-modified porous Ni layers in 0.1 M NaOH and recorded very high values of the j_0, on the order of 7.2×10^{-3} to 1.2×10^{-2} A cm^{-2}. However, these results are definitely overestimated as for all calculations, the authors employed the surface area of an initial, unmodified Ni rotating disk electrode (0.34 cm^2).

Tafel Polarization Curves

Figure 5 illustrates the derived potentiostatic Tafel polarization plots. Thus, the recorded cathodic slopes (b_c) came to 77, 98, and 154 mV dec^{-1} for the SD 1, ED 1, and the etched Ni foam samples, respectively. In addition, the corresponding Tafel-based j_0 parameter values for the HER came to 1.5×10^{-5} (SD 1), 4.1×10^{-5} (ED 1: superior catalytic HER activity), and 3.7×10^{-6} A cm^{-2} (etched Ni foam). It should be stressed here that the Tafel-calculated values of the j_0 parameter are fairly close to those impedance-derived values of the exchange current-density in Fig. 4 (also compared with similar b_c and j_0 values obtained on unmodified and Pd and Ru-activated Ni foam samples in Ref. [14] from this laboratory).

However, it is well known that the exchange current-densities are strongly dependent on the Tafel slope (see, e.g., work by A. Lasia in Ref. [29]), so that a very good way to compare mutual activity of electrodes is to present the overpotential values recorded at the selected current-densities. Therefore, based on Fig. 5, an apparent activity of the catalysts was determined for the current-densities of 1.0 and 0.3 mA cm^{-2}: $\eta_{1.0}$ and $\eta_{0.3}$. Consequently, the obtained results for $\eta_{1.0}$ came to − 434, − 339, and − 266 mV; − 291, − 169, and − 100 mV ($\eta_{0.3}$) for the etched Ni foam, SD 1, and ED 1 electrodes, respectively.

Conclusions

Both spontaneously as well as electrochemically deposited iridium on Ni foam surface (at ca. 0.1–0.3 wt.% Ir) provide highly HER active catalyst materials in 0.1 M sodium hydroxide medium. These catalysts, especially etched Ni foam and electrodeposited ED 1 sample, respectively outperform those of unmodified and Pd/Ru-activated Ni foam materials, produced by an analogous, spontaneous metal deposition route from this laboratory. Most importantly, in this communication, Ni foam electrode provides large surface area catalyst's base for the deposition of small amount of fairly homogeneous and highly active nano-sized iridium deposits (contrast to very large surface area, Ni foam-Pd/Ru entities with nanocatalytic grain structures).

Preliminary HER results presented in this paper clearly indicated considerable opportunities for the employment of Ir-modified (most likely by very small amounts of electrodeposited iridium element) nickel foam cathodes in alkaline water electrolysis.

Funding Information This work has been partly financed by the internal research grant no. 20.610.001-300, provided by The University of Warmia and Mazury in Olsztyn. Mateusz Luba would also like to acknowledge a scholarship from the program Interdisciplinary Doctoral Studies in Bioeconomy (POWR.03.02.00-00-1034/16-00), funded by the European Social Fund.

Open Access This article is licensed under a Creative Commons Attribution 4.0 International License, which permits use, sharing, adaptation, distribution and reproduction in any medium or format, as long as you give appropriate credit to the original author(s) and the source, provide a link to the Creative Commons licence, and indicate if changes were made. The images or other third party material in this article are included in the article's Creative Commons licence, unless indicated otherwise in a credit line to the material. If material is not included in the article's Creative Commons licence and your intended use is not permitted by statutory regulation or exceeds the permitted use, you will need to obtain permission directly from the copyright holder. To view a copy of this licence, visit http://creativecommons.org/licenses/by/4.0/.

References

1. J.Y. Huot, L. Brossard, Int. J. Hydrog. Energy **12**(12), 821 (1987)
2. H.E.G. Rommal, P.J. Morgan, J. Electrochem. Soc. **135**(2), 343 (1988)
3. B.E. Conway, B.V. Tilak, Adv. Catalysis **38**, 1 (1992)
4. H. He, H. Liu, F. Liu, K. Zhou, Surf. Coat. Technol. **201**, 958 (2006)
5. E. Verlato, S. Cattarin, N. Comisso, A. Gambirasi, M. Musiani, L. Vazquez-Gomez, Electrocatalysis **3**, 48 (2012)
6. S. Inazawa, A. Hosoe, M. Majima, K. Nitta, SEI Tech. Rev. **71**, 23 (2010)
7. I. Bianchi, E. Guerrini, S. Trasatti, Chem. Phys. **319**, 192 (2005)
8. L. Vazquez-Gomez, S. Cattarin, P. Guerriero, M. Musiani, Electrochim. Acta **53**, 8310 (2008)
9. P. Kim, J.B. Joo, W. Kim, J. Kim, I.K. Song, J. Yi, J. Power Sources **160**, 987 (2006)
10. B. Beyribey, B. Corbacioglu, Z. Altin, GUJS **22**(4), 351 (2009)
11. Y. Suo, I.M. Hsing, J. Power Sources **196**, 7945 (2011)
12. A. Dutta, S.S. Mahapatra, J. Datta, Int. J. Hydrog. Energy **36**, 14898 (2011)
13. R.M. Modibedi, T. Masombuka, M.K. Mathe, Int. J. Hydrog. Energy **36**, 4664 (2011)
14. B. Pierozynski, T. Mikolajczyk, I.M. Kowalski, J. Power Sources **271**, 231 (2014)
15. B. Pierozynski, T. Mikolajczyk, Electrocatalysis **6**, 51 (2015)
16. B. Pierozynski, T. Mikolajczyk, Int. J. Electrochem. Sci. **10**, 10454 (2015)
17. B. Pierozynski, T. Mikolajczyk, Electrocatalysis **7**, 121 (2016)
18. M. Duca, E. Guerrini, A. Colombo, S. Trasatti, Electrocatalysis **4**, 338 (2013)
19. S.R. Mellsop, A. Gardiner, A.T. Marshall, Electrocatalysis **7**, 226 (2016)
20. A. Papaderakis, N. Pliatsikas, P. Patsalas, D. Tsiplakides, S. Balomenou, A. Touni, S. Sotiropoulos, J. Electroanal. Chem. **808**, 21 (2018)
21. S. Le Vot, L. Roue, D. Belanger, Electrochim. Acta **59**, 49 (2012)
22. J.R. Macdonald, *Impedance spectroscopy, emphasizing solid materials and systems* (John Wiley & Sons, New York, 1987)
23. T. Pajkossy, J. Electroanal. Chem. **364**, 111 (1994)
24. B.E. Conway, B. Pierozynski, J. Electroanal. Chem. **622**, 10 (2008)
25. J.G. Highfield, E. Claude, K. Oguro, Electrochim. Acta **44**, 2805 (1999)
26. R.K. Shervedani, A.R. Madram, Electrochim. Acta **53**, 426 (2007)
27. S. Martinez, M. Metikos-Hukovic, L. Valek, J. Mol. Cat. A: Chem. **245**, 114 (2006)
28. M. Sheng, B. Jiang, B. Wu, F. Liao, X. Fan, H. Lin, Y. Li, Y. Lifshitz, S.T. Lee, M. Shao, ACS Nano **13**(3), 2786 (2019)
29. A. Lasia, Int. J. Hydrog. Energy **44**, 19484 (2019)

Publisher's Note Springer Nature remains neutral with regard to jurisdictional claims in published maps and institutional affiliations.